Progress In Electromagnetics Research C, Vol. 30, 53–64, 2012

EXPERIMENTAL CHARACTERIZATION OF A 434 MHz WIRELESS ENERGY LINK FOR MEDICAL APPLICATIONS

G. Monti*, L. Tarricone, and C. Trane

Department of Innovation Engineering, University of Salento, Via Monteroni, Lecce 73100, Italy

Abstract—This paper presents an experimental study of the performance of a wireless resonant energy link for implantable biomedical devices. More specifically, the proposed system consists of two planar resonators: a primary resonator that is connected to a power source and operates outside the body, and a secondary resonator that is connected to the implanted device and operates inside the body. Each resonator is a planar spiral resonator; the wireless power transmission is obtained by exploiting the magnetic coupling between the two resonators when they are operating at small distances. A prototype working in the ISM band centered at 434 MHz has been developed and analyzed. Reported results confirm that the proposed system is a viable solution for wirelessly providing implantable devices with the power necessary for operation.

1. INTRODUCTION

Over the last decade there has been a growing interest in implantable devices for healthcare sensing and monitoring applications [1–5]. These devices are key components for the treatment of serious diseases such as acute diabetes, epilepsy, heart disease, etc. In the case of acute diabetes, implantable sensors are used for a continuous monitoring of the blood glucose level; for epilepsy and similar neurological disorders the use of programmable brain stimulators avoid surgical operations. In cardiology, implantable sensors are used for the prediction of life threatening episodes.

One of the major challenges of these implantable devices is supplying them with the power necessary to perform operations. Early

Received 26 March 2012, Accepted 24 May 2012, Scheduled 1 June 2012

* Corresponding author: Giuseppina Monti (giuseppina.monti@unisalento.it).

devices used battery-type power sources, such as, for instance, small lithium ion batteries. Although this solution allows the implanted device to work without a physical connection with an external power supply, it has the disadvantage of requiring invasive maintenance operations. In fact, due to the limited lifetime of modern batteries, it is necessary to operate on patients, with consequent risks to the health and additional expenses.

A viable solution to overcome this drawback is to wirelessly supply the necessary power. This can be obtained both by directly providing power to the implantable device or by using rechargeable batteries [6–12]. Introduced by Tesla over a hundred years ago [13], the basic idea of Wireless Power Transmission (WPT) is to wirelessly transmit power without any physical support.

WPT is generally implemented by using resonant systems communicating by means of their electromagnetic field. Two main strategies can be identified depending on whether the communication uses the far or the near electromagnetic field. In a far-field communication, antennas are used to transmit and receive power [14–17]; whereas, in a near-field communication electrically or magnetically coupled systems are used resulting in a so-called Wireless Resonant Energy Link (WREL).

Several recent studies have been dedicated to inductively coupled systems [6, 9–12, 18, 19]. In fact, the use of a magnetic resonant coupling appears to be a promising solution for efficient wireless mid-range energy transfer.

In these systems the WREL is obtained by using three-dimensional coils or planar resonators coupled by their electromagnetic field. In particular, each wireless link consists of at least two resonators connected to the power generator (primary resonator) and to the power end-user (secondary resonator), respectively.

When this approach is used for powering implantable systems, the design is complicated by the fact that the primary resonator operates outside the body, whereas the secondary resonator operates inside the body directly connected to the implantable device [10]. As a consequence, the efficiency of the wireless link is strongly affected by the presence of human tissues. Accordingly, considering that loss due to the presence of human tissues increases with frequency, many near field systems that have been proposed in the literature ([6, 9–12, 20]) operate at frequencies below a few tens of MHz.

In this paper, the power transfer efficiency that can be obtained in the ISM (Industrial, Scientific and Medical) band centered at 434 MHz is experimentally and numerically investigated.

More specifically, a WREL using two segmented planar resonators

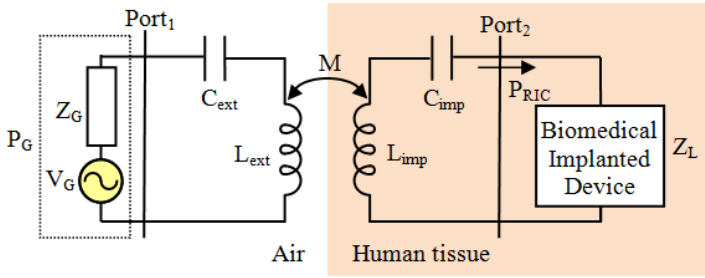

Figure 1. Schematic representation of the inductive link proposed in this paper.

is proposed; results corresponding to tests performed by inserting the secondary resonator in minced pork samples are reported and discussed. Measured data demonstrate the viability of the proposed system in obtaining energy autonomy for implantable devices.

The paper is structured as follows: Section 2 briefly describes the proposed inductive link. Numerical and experimental data are given and discussed in Section 3; finally, some conclusions are drawn in Section 4.

2. PROPOSED INDUCTIVE LINK

The wireless system proposed in this paper for powering implantable devices consists of two planar resonators. A schematic representation of the inductive link is given in Figure 1. Each resonator can be represented as a resonant LC circuit; the primary resonator is connected to a power source while the secondary resonator is placed inside the body and it is connected to an implanted device. The two resonators are inductively coupled so that a current supplied to the primary resonator induces a current in the secondary resonator.

As for the geometry of the planar resonator here proposed, it is illustrated in Figure 2(a). It consists of two segmented spiral loops realized on the top and bottom face of a low-cost FR4 substrate ($\varepsilon_r = 3.7$, $\tan(\delta) = 0.025$) with a thickness of 1.6 mm.

Each loop is a mirrored copy of the other one. The use of a segmented spiral in designing the loops allows to achieve an in-phase current distribution along each spiral even when its perimeter is comparable with the operating wavelength [18, 19]. This way, a strong and uniform magnetic field is generated over the internal zone of the loop.

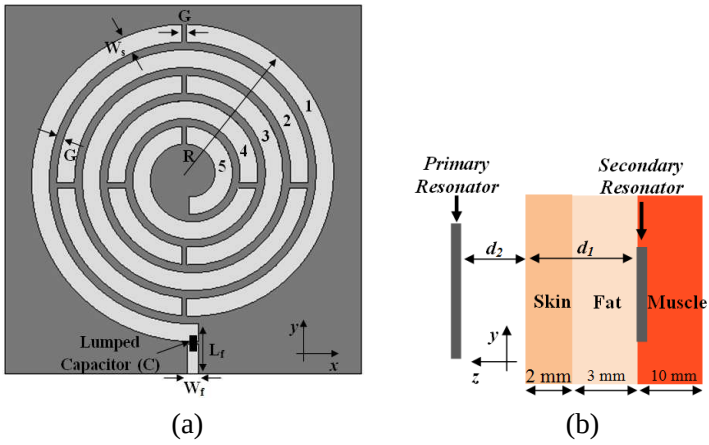

Figure 2. (a) Geometry of the segmented spiral loop resonator. (b) Configuration adopted in full-wave simulations for the optimization of the inductive link. The secondary resonator was placed inside a stratified medium consisting of three layers (skin, fat and muscle).

Furthermore, the loop on the top face of the FR4 substrate is loaded with a lumped capacitor (a surface mounted capacitor EIA 0805 of Johanson Technology); the presence of this capacitor simplifies the loop design with respect to a given resonance frequency and input impedance.

Referring to the parameters illustrated in Figure 2(a), the primary and the secondary loops have been optimized in order to be matched with respect to a 50 Ω impedance and to work in the ISM (Industrial, Scientific and medical) band centered at 433.92 MHz. The number of spiral turns was also optimized. The simulator CST Microwave Studio was used for full-wave simulations and optimizations. Simulations were performed by taking into account the presence of a biocompatible coating on all the substrate surfaces. More specifically, the coating was a layer of parylene C with a dielectric constant of 3.15 and a thickness of 1 μm.

First we optimized each single resonator, and then full-wave simulations and optimizations were performed by considering the overall inductive link (that is the system schematized in Figure 1).

Referring to applications that use devices implanted under the skin to a depth of 0.5 cm, the parameters of the secondary resonator were optimized by considering the resonator inserted in a stratified medium consisting of the following three layers: a first layer of skin, a second layer of fat and a third layer of muscle. Details about the parameters

Table 1. Parameters of the stratified medium adopted in full-wave simulations.

		Relative electric permittivity (ε_r)	Conductivity [S/m]	Thickness [mm]
Layer 1	Skin	46.78	0.68	2
Layer 2	Fat	5.56	0.0416	3
Layer 3	Muscle	56.87	0.8048	10

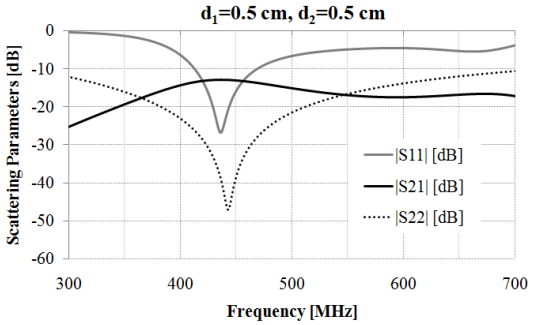

Figure 3. Scattering parameters calculated by means of full-wave simulations for the inductive link configured as in Figure 2(b). Port 1 and port 2 are connected to the primary and the secondary resonator, respectively.

assumed for each layer are given in Table 1 [21–23]. As illustrated in Figure 2(b), the secondary resonator was placed between layers 2 and 3. Results obtained this way are given in the next section and compared with experimental data.

3. NUMERICAL AND EXPERIMENTAL RESULTS

Referring to Figure 2(a), Table 2 summarizes the dimensions of the loops calculated by means of full-wave optimization in order to have a working frequency in the ISM band centered at 434 MHz. The primary resonator is a 5-turn segmented spiral and occupies an area of $(67.5 \times 69.3)\,\mathrm{mm}^2$, while the secondary resonator is a 3-turn segmented spiral and occupies an area of $(32.3 \times 34.1)\,\mathrm{mm}^2$. Figure 3 shows the scattering parameters (S-parameters) calculated when the primary and the secondary resonators are configured as illustrated in Figure 2(b) with $d = 1\,\mathrm{cm}$ ($d_1 = 0.5\,\mathrm{cm}$, $d_2 = 0.5\,\mathrm{cm}$); the port numbering is the one illustrated in Figure 1. The value calculated at 434 MHz for the S_{21} parameter is of about $-12.8\,\mathrm{dB}$.

A prototype of each resonator was realized by using photolithographic techniques, photographs are given in Figure 4. The R&S® ZVL6 vector network analyzer (Rohde & Schwarz) was used to perform scattering parameters measurements.

Table 2. Parameters of the spiral resonators calculated by means of full-wave optimizations. All dimensions are in millimeters.

Primary Resonator (5-turn), lumped capacitor (C) = 20 pF					
R	G	W_s	G_s	L_f	W_f
29.5	1.5	3.33	0.92	9.3	2
Secondary Resonator (3-turn), lumped capacitor (C) = 22 pF					
R	G	W_s	G_s	L_f	W_f
13.5	1.9	1.9	0.47	4.4	1.9

Figure 4. Photographs of the realized resonators.

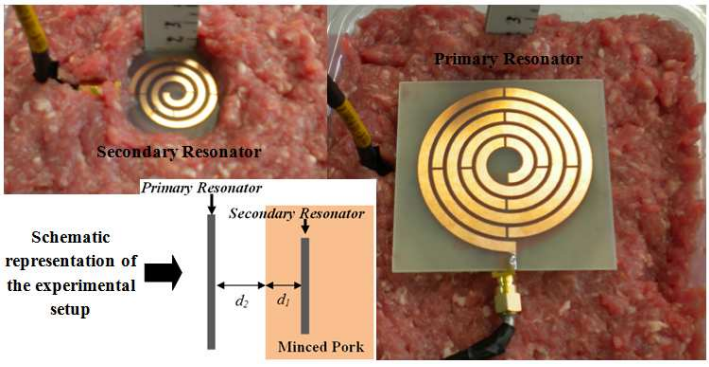

Figure 5. Experimental setup adopted to verify the performance of the proposed inductive link in presence of human tissues.

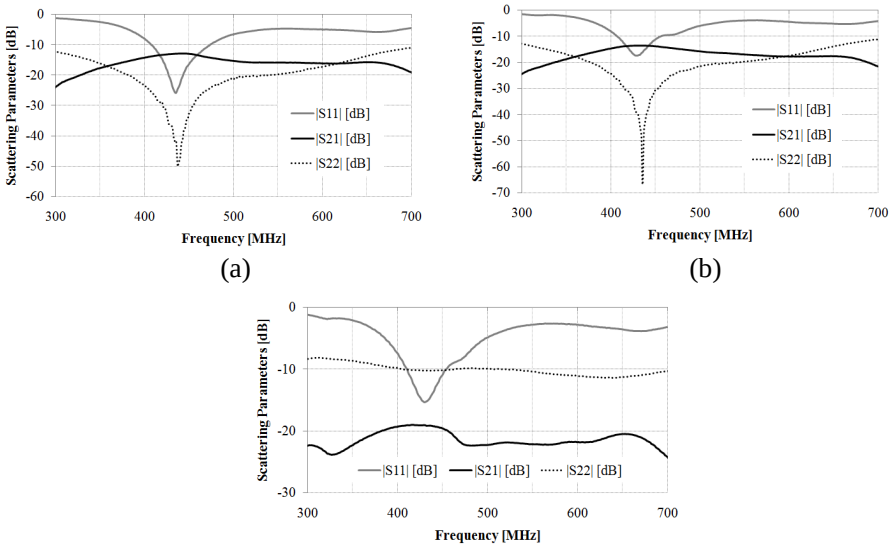

Figure 6. S-parameters measured by using the experimental setup illustrated in Figure 5. Measurements were performed for different values of the distance between the two resonators: (a) 1 cm ($d_1 = 0.5$ cm, $d_2 = 0.5$ cm), (b) 1.5 cm ($d_1 = 0.5$ cm, $d_2 = 1.0$ cm), (c) 2 cm ($d_1 = 0.5$ cm, $d_2 = 0.5$ cm).

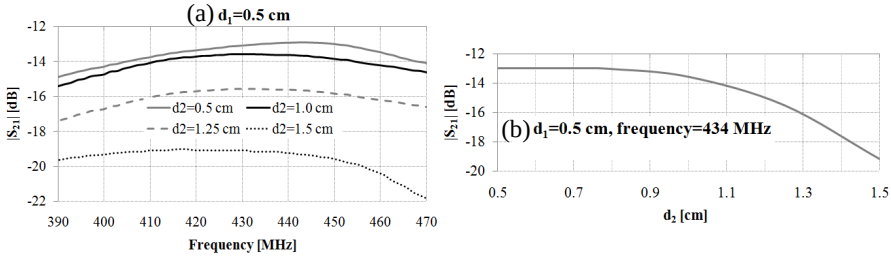

Figure 7. Measured data of the S_{21} parameter for different values of d_2.

In order to experimentally evaluate the performance of the proposed inductive link in the presence of human tissues, we used minced pork [8]. In fact, in the frequency range of interest minced pork exhibits values of electric parameters very close to the ones corresponding to the human skin and muscle [8, 21–23].

The experimental setup adopted for measurements is illustrated in Figure 5; the secondary resonator was placed inside minced pork at a depth d_1, while the primary resonator was placed at a distance d_2 with respect to the minced pork surface. As a consequence, the overall distance between the two resonators was $d = d_1 + d_2$ (see Figure 5).

Figures 6–7 illustrate the S-parameters measured for different values of the distance between the two resonators. More specifically, measurements were performed with the secondary resonator placed at a fixed depth of 0.5 cm ($d_1 = 0.5$ cm), while the distance of the primary resonator with respect to the minced pork surface (d_2) was varied. In the case of a distance between the two resonators of 1 cm ($d_1 = 0.5$ cm, $d_2 = 0.5$ cm), a maximum of -12.9 dB at 443 MHz was measured for the S_{21} parameter (see Figure 6(a)). As for the frequencies of resonance, from measurements the primary and the secondary resonator resonate at 435.6 MHz and at 437.1 MHz, respectively. However, the measured S_{11} and S_{22} assume values lower than -20 dB over the whole frequency range of the ISM band [433 MHz, 434.79 MHz]. More in detail, at the center of this band ($\sim$ 434 MHz) the following values were measured: $S_{11} = -25.66$ dB, $S_{22} = -41.8$ dB, $S_{21} = -12.9$ dB. The measured S-parameters given in Figure 6(a) were converted to Z-parameters and used to calculate the mutual inductance of the proposed wireless link [10]. This way, an inductance of 34.47 nH (L_{ext}) and of 7.88 nH (L_{imp}) was calculated for the primary and secondary resonator, respectively; the value calculated for the mutual inductance was 0.692 nH, thus corresponding to a mutual coupling (M) of 0.042 ($M = L_M/\sqrt{L_{ext}L_{imp}}$).

Figure 7 summarizes results obtained for different values of d_2; it can be noticed that for values of d_2 greater than 1.2 cm the measured S_{21} is lower than -15 dB. As evident from Figure 6(c), this is mainly due to the fact that the level of matching of the primary and secondary resonator with respect to a 50 Ω impedance worsens when the distance between the two resonators increases.

As for the power transfer efficiency (η), referring to Figure 1, η can be calculated from S-parameters by using the following formula:

$$\eta\,[\%] = \frac{P_{RIC}}{P_G} \times 100, \quad P_{RIC} = P_G\,|S_{21}|^2 \left(1 - |S_{11}|^2\right) \left(1 - |S_{22}|^2\right) \quad (1)$$

From measurements, at 434 MHz the power transfer efficiency of the proposed wireless link is 5.1% when the resonators are at a distance of 1 cm ($d_1 = d_2 = 0.5$ cm). This means that, if the power supplied by the transmitter to the primary resonator is 1 W (i.e., $P_G = 1$ W), the power delivered by the secondary resonator to the implantable device (P_{RIC}) is 51 mW. These results are summarized in Figure 8 where the values of P_{RIC} calculated for different values of d_2 are reported.

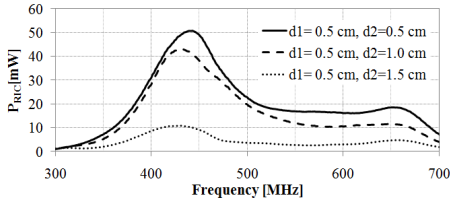

Figure 8. P_{RIC} (i.e., power delivered by the secondary resonator to the implantable device) calculated by using Equation (1) and the measured values of the scattering parameters.

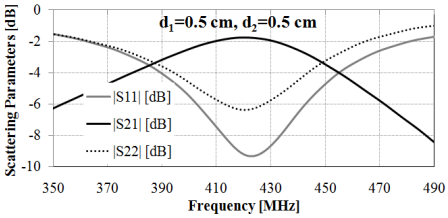

Figure 9. Simulation results obtained by using the configuration illustrated in Figure 3 and by setting the conductivity of the three human layers (tissue, fat and muscle) equal to zero. The layers permittivity and thickness are the ones given in Table 1.

Considering that the typical power consumption of many implantable devices is between hundred of μW and a few mW [24] and assuming a value of 1 W for P_G, the maximum distance between the primary and the secondary resonator that allows the use of the proposed wireless link for the powering of these devices is of about 2 cm. In fact, from measurements and by using (1), it can be derived that the proposed link is able to deliver a power of 43 mW when d is equal to 1.5 cm ($d_1 = 0.5$ cm, $d_2 = 1.0$ cm) and a power of 10 mW when d is equal to 2 cm ($d_1 = 0.5$ cm, $d_2 = 1.5$ cm).

The effects of the human tissues on the performance of the proposed wireless link was also investigated, corresponding results are given in Figures 9–10. In particular, Figure 9 shows the S-parameters calculated by means of full-wave simulations by using the configuration illustrated in Figure 2(b) and by setting the conductivity of the three human layers equal to zero. The layers permittivity and thickness assumed in simulations were the ones given in Table 1. From simulations, neglecting the conductivity of the human layers results into a slight shift of the frequency of resonance (both resonators resonate approximately at 420 MHz). As for the values of the S-

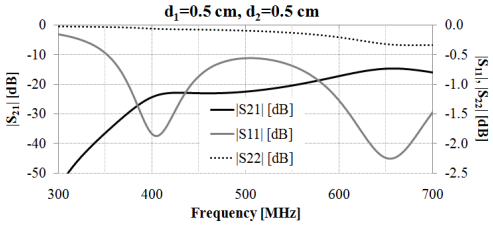

Figure 10. Simulation results corresponding to the proposed wireless inductive link when both resonators are placed in air.

parameters, it can be noticed that the level of matching with respect to a 50 Ω impedance worsens; nonetheless, a maximum of about −1.77 dB was calculated for S_{21}. More specifically, by using (1) the simulated values of the S-parameters correspond to a maximum of the power transfer efficiency of about 45%.

Finally, Figure 10 shows the S-parameters corresponding to the proposed inductive link when both resonators are placed in air at a distance of 1 cm. In this case, due to the fact that the frequency of resonance of the secondary resonator shifts towards higher frequencies (it becomes approximately equal to 750 MHz), the performance of the link was degraded completely.

4. CONCLUSIONS

In this paper, an inductive link for medical applications working in the ISM (Industrial, Scientific and Medical) band centered at 434 MHz has been investigated. The proposed wireless link consists of two segmented spiral resonators; numerical and experimental results have been reported and discussed. Tests were performed by inserting the resonator to be connected to the implantable device in a minced pork. Experimental and numerical data demonstrate that the approach here proposed is a viable solution to wirelessly power implantable devices.

REFERENCES

1. Laerhoven, K. V., B. P. L. Lo, et al., "Medical healthcare monitoring with wearable and implantable sensors," *International Workshop on Ubiquitous Computing for Pervasive Healthcare Applications (UbiHealth)*, 2004.
2. Park, D. J., Y. J. Lee, and J. Y. Park, "Long-term stabled non-enzymatic glucose sensor for continuously monitoring system

applications," *Proc. of the IEEE Nano/Micro Engineered and Molecular Systems*, 704–707, China, 2008.

3. Salam, M. T., D. K. Nguyen, and M. Sawan, "A low-power implantable device for epileptic seizure detection and neurostimulation," *Proc. of IEEE Biomedical Circuits and Systems Conference (BioCAS)*, 154–157, Paphos, Cyprus, 2010.
4. Vidal, N., S. Curto, J. M. Lopez-Villegas, J. Sieiro, and F. M. Ramos, "Detuning study of implantable antennas inside the human body," *Progress In Electromagnetics Research*, Vol. 124, 265–283, 2012.
5. Gemio, J., J. Parron, and J. Soler, "Human body effects on implantable antennas for ism bands applications: Models comparison and propagation losses study," *Progress In Electromagnetics Research*, Vol. 110, 437–452, 2010.
6. Ashoori, E., F. Asgarian, et al., "Design of double layer printed spiral coils for wirelessly-powered biomedical implants," *Proc. of Engineering in Medicine and Biology Society*, 2882–2885, Boston, Massachusetts, 2011.
7. Goto, K., T. Nakagawa, and S. Kawata, "An implantable power supply with an optically rechargeable lithium battery," *IEEE Trans. Biomed. Eng.*, Vol. 48, No. 7, 830–833, 2001.
8. Huang, F. J., C. M. Lee, et al., "Rectenna application of miniaturized implantable antenna design for triple-band biotelemetry communication," *IEEE Trans. on Antennas and Propagation*, Vol. 59, No. 7, 2646–2653, 2011.
9. Laskovski, A. N., M. R. Yuce, and T. Dissanayake, "Stacked spirals for biosensor telemetry," *IEEE Sensor Journal*, Vol. 11, No. 6, 1484–1490, 2011.
10. Jow, U. M. and M. Ghovanloo, "Modeling and optimization of printed spiral coils in air, saline, and muscle tissue environments," *IEEE Trans. on Biomedical Circuits and Systems*, Vol. 3, No. 5, 339–347, 2009.
11. Jung, K. H., Y. H. Kim, et al., "Wireless power transmission for implantable devices using inductive component of closed magnetic circuit," *Electronics Letters*, Vol. 45, No. 1, 21–22, 2009.
12. Kumar, A., S. Mirabbasi, and M. Chiao, "Resonance-based wireless power delivery for implantable devices," *Proc. of IEEE Biomedical Circuits and Systems Conference*, 25–28, Beijing, China, 2009.
13. Tesla, N., "Apparatus for transmitting electrical energy," U.S. Patent, 1119732, 1914.

14. Monti, G. and F. Congedo, "UHF rectenna using a bowtie antenna," *Progress In Electromagnetics Research C*, Vol. 26, 181–192, 2012.
15. Monti, G., L. Tarricone, and M. Spartano, "X-band planar rectenna," *Antennas and Wireless Propagation Letters*, Vol. 10, 1116–1119, 2011.
16. Vidal, N., S. Curto, J. M. Lopez-Villegas, J. Sieiro, and F. M. Ramos, "Detuning study of implantable antennas inside the human body," *Progress In Electromagnetics Research*, Vol. 124, 265–283, 2012.
17. Gemio, J., J. Parron, and J. Soler, "Human body effects on implantable antennas for ism bands applications: Models comparison and propagation losses study," *Progress In Electromagnetics Research*, Vol. 110, 437–452, 2010.
18. Li, X. and L. Cao, "Microstrip-based segmented coupling reader antenna for near-field RFID applications," *Microwave and Optical Technology Lett.*, Vol. 53, No. 8, 1774–1777, 2011.
19. Qing, X. and Z. N. Chen, "Segmented spiral antenna for UHF near-field RFID," *Proc. of IEEE Int. Symp. on Antennas and Propagation APSURSI*, 996–999, 2011.
20. Poon, A. S. Y., S. O'Driscoll, and T. H. Meng, "Optimal operating frequency in wireless power transmission for implantable devices," *Proc. of the 29th Int. Conf. of the IEEE Eng. in Medicine and Biology Society*, Lyon, France, Aug. 23–26, 2007.
21. Gabriel, C., S. Gabriel, and E. Corthout, "The dielectric properties of biological tissues: I. Literature survey," *Phys. Med. Biol.*, Vol. 41, 2231–2249, 1996.
22. Gabriel, S., R. W. Lau, and C. Gabriel, "The dielectric properties of biological tissues: II. Measurements in the frequency range 10 Hz to 20 GHz," *Phys. Med. Biol.*, Vol. 41, 2251–2269, 1996.
23. Gabriel, S., R. W. Lau, and C. Gabriel, "The dielectric properties of biological tissues: III. Parametric models for the dielectric spectrum of tissues," *Phys. Med. Biol.*, Vol. 41, 2271–2293, 1996.
24. Oh, J. H., T. H. Kim, J. H. Yoo, J. K. Pack, Y. M. Yoon, M. Y. Choi, and S. Y. Lee, "Human exposure assessment for wireless power transmission system," *PIERS Proceedings*, Xi'an, China, Mar. 22–26, 2010.